

This article was downloaded by: [Columbia University HHMI]

On: 19 February 2009

Access details: Access Details: [subscription number 791575380]

Publisher Informa Healthcare

Informa Ltd Registered in England and Wales Registered Number: 1072954 Registered office: Mortimer House, 37-41 Mortimer Street, London W1T 3JH, UK



## International Journal of Radiation Biology

Publication details, including instructions for authors and subscription information:

<http://www.informaworld.com/smpp/title-content=t713697337>

### Evaluation of lesion clustering in irradiated plasmid DNA

C. Leloup <sup>a</sup>; G. Garty <sup>a</sup>; G. Assaf <sup>a</sup>; A. Cristovão <sup>a</sup>; A. Breskin <sup>a</sup>; R. Chechik <sup>a</sup>; S. Shchemelinin <sup>a</sup>; T. Paz-Elizur <sup>b</sup>; Z. Livneh <sup>b</sup>; RW Schulte <sup>c</sup>; V. Bashkirov <sup>c</sup>; JR Milligan <sup>d</sup>; B. Grosswendt <sup>e</sup>

<sup>a</sup> Dept. of Particle Physics, Weizmann Institute of Science, Rehovot, Israel <sup>b</sup> Dept. of Biological Chemistry, Weizmann Institute of Science, Rehovot, Israel <sup>c</sup> Dept. of Radiation Medicine, Loma Linda University Medical Center, Loma Linda, USA <sup>d</sup> Dept. of Radiology, University of California at San Diego, La Jolla, USA <sup>e</sup> Physikalisch Technische Bundesanstalt, D-38116 Braunschweig, Germany

Online Publication Date: 01 January 2005

**To cite this Article** Leloup, C., Garty, G., Assaf, G., Cristovão, A., Breskin, A., Chechik, R., Shchemelinin, S., Paz-Elizur, T., Livneh, Z., Schulte, RW, Bashkirov, V., Milligan, JR and Grosswendt, B.(2005)'Evaluation of lesion clustering in irradiated plasmid DNA',International Journal of Radiation Biology,81:1,41 — 54

**To link to this Article:** DOI: 10.1080/09553000400017895

**URL:** <http://dx.doi.org/10.1080/09553000400017895>

## PLEASE SCROLL DOWN FOR ARTICLE

Full terms and conditions of use: <http://www.informaworld.com/terms-and-conditions-of-access.pdf>

This article may be used for research, teaching and private study purposes. Any substantial or systematic reproduction, re-distribution, re-selling, loan or sub-licensing, systematic supply or distribution in any form to anyone is expressly forbidden.

The publisher does not give any warranty express or implied or make any representation that the contents will be complete or accurate or up to date. The accuracy of any instructions, formulae and drug doses should be independently verified with primary sources. The publisher shall not be liable for any loss, actions, claims, proceedings, demand or costs or damages whatsoever or howsoever caused arising directly or indirectly in connection with or arising out of the use of this material.

## Evaluation of lesion clustering in irradiated plasmid DNA

C. LELOUP<sup>1</sup>, G. GARTY<sup>1</sup>, G. ASSAF<sup>1</sup>, A. CRISTOVÃO<sup>1</sup>, A. BRESKIN<sup>1</sup>, R. CHECHIK<sup>1</sup>,  
S. SHCHEMELININ<sup>1</sup>, T. PAZ-ELIZUR<sup>2</sup>, Z. LIVNEH<sup>2</sup>, R. W. SCHULTE<sup>3</sup>, V. BASHKIROV<sup>3</sup>,  
J. R. MILLIGAN<sup>4</sup>, & B. GROSSWENDT<sup>5</sup>

<sup>1</sup>Dept. of Particle Physics, Weizmann Institute of Science, Rehovot, 76100, Israel, <sup>2</sup>Dept. of Biological Chemistry, Weizmann Institute of Science, Rehovot, 76100, Israel, <sup>3</sup>Dept. of Radiation Medicine, Loma Linda University Medical Center, Loma Linda, CA 92354, USA, <sup>4</sup>Dept. of Radiology, University of California at San Diego, La Jolla, CA 92093, USA and <sup>5</sup>Physikalisch Technische Bundesanstalt, D-38116 Braunschweig, Germany

(Received 11 March 2004; accepted 29 September 2004)

### Abstract

**Purpose:** To measure the yield of DNA strand breaks and clustered lesions in plasmid DNA irradiated with protons, helium nuclei, and  $\gamma$ -rays.

**Materials and methods:** Plasmid DNA was irradiated with 1.03, 19.3 and 249 MeV protons (linear energy transfer = 25.5, 2.7, and 0.39 keV  $\mu\text{m}^{-1}$  respectively), 26 MeV helium nuclei (25.5 keV  $\mu\text{m}^{-1}$ ) and  $\gamma$ -rays (<sup>137</sup>Cs or <sup>60</sup>Co) in phosphate buffer containing 2 mM or 200 mM glycerol. Single- and double-strand breaks (SSB and DSB) were measured by gel electrophoresis, and clustered lesions containing base lesions were quantified by converting them into irreparable DSB in transformed bacteria.

**Results:** For protons, SSB yield decreased with increasing LET (linear energy transfer). The yield of DSB and all clustered lesions seemed to reach a minimum around 3 keV  $\mu\text{m}^{-1}$ . There was a higher yield of SSB, DSB and total clustered lesions for protons compared to helium nuclei at 25.5 keV  $\mu\text{m}^{-1}$ . A difference in the yields between <sup>137</sup>Cs and <sup>60</sup>Co  $\gamma$ -rays was also observed, especially for SSB.

**Conclusion:** In this work we have demonstrated the complex LET dependence of clustered-lesion yields, governed by interplay of the radical recombination and change in track structure. As expected, there was also a significant difference in clustered lesion yields between various radiation fields, having the same or similar LET values, but differing in nanometric track structure.

### Introduction

Ionizing radiation is known to cause many different types of lesions in DNA, most importantly base oxidations, abasic sites, strand breaks and DNA protein cross links (Ward 1988). An additional level of complexity is added by the fact that these lesions are not randomly distributed but are clustered both at the local DNA level (within 10–20 base pairs) and at the regional level of higher-order chromatin structures (Rydberg 2001). These clustered lesions are believed to be difficult to repair and may, therefore, be responsible for mutations and cell death (Belli et al. 1996, Pastwa et al. 2003).

For our basic understanding of radiation interaction with DNA it is essential to study in detail how the frequency and complexity of DNA lesions depends on radiation quality. Our current knowledge on this subject is mostly based on experimental studies of strand breaks and base damage yields in cells and DNA model systems as a function of linear energy transfer (LET) for various forms of ionizing radiation as well as on theoretical biophysical models.

Experimental results of the LET dependence of the yield of double-strand breaks (DSB) in eukaryotic cells have been controversial. Most experimental studies reported either a relatively weak

or no dependence of the DSB yield on LET, depending on the method used (Prise et al. 1998, 2001; Belli et al. 2002). Thus the reported LET dependence for DSB induction has been much lower than that for cell killing. It is now believed that current techniques of DSB measurement in cells underestimate the true yield of DSBs (Prise et al. 2001), which may at least partially explain this discrepancy.

Over the last three decades, simple experimental model systems of viral or plasmid DNA have been used to study the LET dependence of DNA lesion formation. Some studies, performed in highly protective solutions to simulate the high free radical scavenging capacity of the cellular environment, reported a reduction of single-strand break (SSB) yields with increasing LET, while the yield of DSB increased up to a maximum at around 500 keV  $\mu\text{m}^{-1}$  (Christensen et al. 1972; Taucher-Scholz 1992). Other studies were typically performed at low scavenging concentrations to avoid the problem of large doses and long irradiation times needed for high scavenging conditions. These studies, which generally showed a decreasing efficiency of both SSB and DSB production with LET (Roots et al. 1990; Taucher-Scholz 1992, 1999) are not necessarily representative for the highly protective cellular environment.

More recently, several investigators have studied the increase in the number of SSB and DSB after incubation of naked DNA irradiated in low-scavenging solutions with base excision repair enzymes (Prise et al. 1999; Milligan et al. 2000, 2001; Sutherland et al. 2001; Gulston et al. 2002). These studies have clearly indicated that many SSB (and also probably DSB) are associated with additional base damage and, therefore, constitute clustered lesions that are more complex than simple SSB or DSB. In addition, these studies have shown that there are clustered lesions consisting only of damaged bases. Clustered lesions are formed by both low- and high-LET radiation, and non-DSB clusters appear to be more common than DSB clusters, in particular for low-LET radiation (Sutherland et al. 2001).

In the last 20 years, many Monte Carlo (MC) studies have been performed simulating the interaction of electrons, protons, alpha particles, and ultra-soft X-rays with DNA in various configurations (Nikjoo et al. 1999, 2001, 2002a, 2002b; Bernhardt et al. 2002; Watanabe and Saito 2002; Friedland et al. 2002, 2003). The results of these studies indicate that DNA lesions may vary widely in their degree of local clustering, ranging from isolated to multiple lesions occurring over a distance of about 10 bp. Moreover, these studies have shown that besides the average ionization density, represented by LET,

track structure influences the number and complexity of different lesion types.

We present here the results of our experimental studies of strand breaks and clustered lesions (including damaged bases) in plasmid DNA. Plasmids were irradiated with protons in the LET range of 0.39–25.5 keV  $\mu\text{m}^{-1}$ , with helium nuclei of 25.5 keV  $\mu\text{m}^{-1}$ , as well as with  $^{60}\text{Co}$  and  $^{137}\text{Cs}$   $\gamma$ -rays. We performed irradiation under both low and high scavenging conditions (2 mM and 200 mM glycerol).

## Materials and Methods

### Plasmid purification

Plasmid DNA pHAZE (Lutze and Winegar 1990) was propagated in *E. coli* XL2-Blue MRF<sup>+</sup> bacteria and purified using Qiagen tip – 500 columns (Qiagen, Valencia, CA, USA) followed by a 60–72 h density gradient centrifugation at 112,504 *g* with 1 g cesium chloride and 0.1 ml ethidium bromide per ml plasmid solution. Plasmid DNA was dialyzed against TE buffer (10 mM Tris-HCl, 1 mM EDTA (ethylene diamine tetra-acetic acid), pH 8), and further purified by gel filtration chromatography with Sephacryl S1000 Superfine (Amersham-Pharmacia, Piscataway, NJ, USA) in TE/1 M sodium chloride buffer. Plasmid DNA was then subjected to diafiltration with 10 mM phosphate buffer, pH 7, using Centriplus-YM 100 ultrafiltration units (Amicon, Millipore, Bedford, MA, USA).

### Irradiation setup

Before irradiation, plasmid DNA was diluted to 1  $\mu\text{g}/\mu\text{l}$ . We have measured DNA damage yields in plasmids irradiated in a solution containing 200 mM glycerol which has a scavenging capacity of  $3.8 \times 10^8 \text{ s}^{-1}$  (Klimczak et al. 1993), similar to that of the cellular environment. Glycerol was used as a scavenger rather than DMSO (dimethyl sulfoxide) since secondary radicals derived from it are unreactive with DNA (Milligan et al. 1996a). In these conditions, the contribution of the direct effect is about 35% of the total effect (Chapman et al. 1973). We also irradiated plasmids in a low scavenging capacity environment, i.e., in the presence of 2 mM glycerol (scavenging capacity of  $3.8 \times 10^6 \text{ s}^{-1}$ , Klimczak et al. 1993) where the indirect effect (mediated mostly through the production of OH radicals) contributes approximately 99% of the total damage. The relative contribution of the indirect effect was estimated by comparing the SSB yields due to the direct effect:  $2 \times 10^{-10} \text{ Gy}^{-1} \text{ Da}^{-1}$  (Milligan et al. 1993), with the yields obtained for 1 or 100 mM DMSO (which corre-

sponds to the scavenging capacity of 2 and 200 mM glycerol):  $1.3 \times 10^{-8} \text{ Gy}^{-1} \text{ Da}^{-1}$  and  $6 \times 10^{-10} \text{ Gy}^{-1} \text{ Da}^{-1}$ , respectively (Milligan et al. 1996b, Figure 4).

For irradiation at different doses, plasmid DNA was divided into aliquots of 5  $\mu\text{l}$  except for 1.03 MeV proton irradiations that were done with 3  $\mu\text{l}$  samples to reduce the sample thickness and minimize energy degradation of the beam within the sample. Gamma irradiations as well as high-energy proton (249 MeV) irradiations of 5  $\mu\text{l}$  DNA samples were performed in 1.5 ml polypropylene tubes. For lower energy proton and helium nuclei irradiations we have constructed an irradiation setup based on the one described by Bashkirov and Schulte (2002), consisting of an air-filled parallel plate ionization chamber (ICRU 1998) for beam dosimetry and a dedicated sample holder (Figure 1). The sample holder enabled spreading the plasmid solution to a thin film (approximately 10  $\mu\text{m}$  sample thickness for 1.03 MeV proton irradiations and 16 mm thickness for 19.3 MeV protons and 26 MeV helium nuclei) between a quartz disc of 2 cm diameter and a foil (Mylar<sup>®</sup> 6  $\mu\text{m}$  or Teflon<sup>®</sup> of 12.7  $\mu\text{m}$  thickness). The sample holder, containing some buffer droplets, was sealed to prevent sample evaporation during long irradiations. All irradiations were performed at 20–22°C.

Dosimetry for the ion irradiations was performed using an air-filled ionization chamber (1  $\mu\text{m}$  thick aluminized Mylar electrodes, 1.6 mm gap) operated without gain but at sufficiently high voltage (300 V) to efficiently collect all charges formed within it. The dose in the sample was calculated according to the guidelines in ICRU 1998, taking into account the area of the beam (about 4 cm<sup>2</sup>), which was slightly smaller than that of the chamber but larger than that

of the DNA sample. The current generated in the ionization chamber (typically 3nA) was integrated using a calibrated digital current integrator (EG&G Ortec model 439) connected to a scaler. Different chambers and charge integrators were used at Weizmann Institute of Sciences (WIS) (1.03 and 19.3 MeV protons as well as the helium nuclei) and at Loma Linda University Medical Center (LLUMC) (250 MeV protons).

Dosimetry for  $\gamma$ -irradiation was performed with a Fricke dosimeter. Aliquots of 5  $\mu\text{l}$  of freshly prepared solution ( $10^{-3}$  M ferrous sulfate,  $10^{-3}$  M sodium chloride and 0.4 M sulfuric acid) were irradiated in the same conditions as the samples. Aliquots were combined and optical density at 304 nm was measured at 25°C immediately after irradiation. The dose absorbed by the sample was calculated using equation 3.31 in Spinks and Woods (1976). For <sup>137</sup>Cs irradiation, the dose rate was also measured with an ionization chamber and a current flow across a PN junction (diode). Both measurements were in agreement with the Fricke dosimetry. For <sup>60</sup>Co irradiation, the dose rate measured with the Fricke dosimeter were 10% higher than the dose rate measured with an ionization chamber. The values from the Fricke dosimetry were chosen because the irradiation setup was the same as that used for DNA.

The 1.03 MeV proton irradiations were performed with the 2.5 MV Van de Graaff accelerator and the 19.3 MeV protons and helium nuclei irradiations were performed with the 14UD Pelletron, both at the Weizmann Institute of Science's accelerator laboratory. The 249 MeV proton irradiations were performed with the proton synchrotron of the Loma Linda University Medical Center. Gamma irradiations were performed with <sup>60</sup>Co (Gamma Cell 150, MDS Nordion, Canada) at WIS and with <sup>137</sup>Cs (Shepherd MarkII) at the University of California at San Diego (UCSD). The maximal average dose rate was 10 Gy min<sup>-1</sup> (with momentary fluctuations up to a factor of two for the accelerator irradiations). The dose rate was kept low in order to prevent oxygen depletion. For  $\gamma$ -irradiation, samples were reoxygenated every 400 Gy. Samples for 249 MeV proton irradiation were irradiated in a tube as well but not reoxygenated. For the 19.3 and 1.03 MeV protons and for the helium nuclei measurements we expect little oxygen depletion due to the large surface area of the plasmid sample and the fact that we flowed dry air over it. It should be noted that Jones et al. (1993) did not see oxygen deprivation for long exposures using a device similar to the device we used for the latter irradiations. In the case that despite our precautions, samples underwent partial oxygen depletion at high doses (this possibility is discussed in paragraph 4.2.) the effect on damages yield should be small since the presence of glycerol

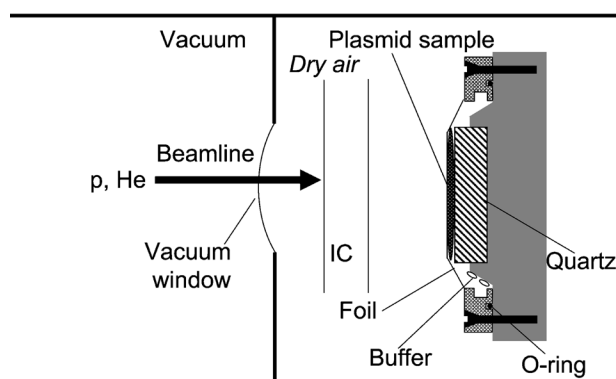


Figure 1. Schematic of the DNA sample holder for irradiation with protons and helium nuclei. The plasmid solution is spread between a foil (Mylar<sup>®</sup> or Teflon<sup>®</sup>) and a quartz substrate. A few buffer droplets maintain humidity in the atmosphere around the plasmid solution. The accelerated charged particles traverse a thin vacuum window (12.7  $\mu\text{m}$  Kapton<sup>®</sup>), cross an ionization-chamber (IC) dosimeter and irradiate the DNA through the thin Mylar<sup>®</sup> or Teflon<sup>®</sup> foil.

minimizes the difference in damage yield between oxygenated and anoxic conditions (Jones et al. 1993; Milligan and Ward 1994; Ayene et al. 1995). Since a source of systematic error could be the fact that irradiations were performed at different institutions, irradiated samples were shipped from one institution to the other and their analysis was repeated. This double analysis gave very similar results. Moreover the irradiation with  $^{60}\text{Co}$  was repeated at the Loma Linda University Medical Center and the results (not shown) were very similar.

The LET values and ranges in water for the radiation qualities used in this study are given in Table I; LET values for protons and helium nuclei were taken from the PSTAR and ASTAR (proton- and alpha-particle stopping and range) databases, (Berger 1995) respectively. The mean LET values for the  $^{60}\text{Co}$  and  $^{137}\text{Cs}$  irradiations were estimated by dividing the mean energy of secondary electrons (586 keV and 252 keV, respectively) by their range in liquid water (2194  $\mu\text{m}$  and 637  $\mu\text{m}$ , respectively), using the data from the NIST (National Institute of Standards and Technology) ESTAR (electron stopping and range) database (Berger 1995). The mean energy of secondary electrons was calculated by dividing the mass energy absorption coefficient (NIST) by the mass attenuation coefficient (NIST) and multiplying by the photon energy.

Plasmid DNA was irradiated at ten to twenty different doses, ranging from 0 to 1000 Gy for 2 mM glycerol solutions and from 0 to 5000 Gy for 200 mM glycerol solutions.

#### Gel electrophoresis assay

Plasmid DNA was kept at 4°C and analyzed within a few hours to a few days after irradiation by standard agarose gel electrophoresis for the relative amount of supercoiled (SC), open-circular (OC), and linear (L) forms. The fragmented (F) form could not be reliably quantified. Diluted samples of 100 ng plasmid (5  $\mu\text{l}$ ) were mixed to loading buffer  $\times$  6 (3  $\times$  TBE buffer, 60% glycerol, 0.6% sodium

dodecyl sulfate, 0.06% bromophenol blue). Gels were run at 30 V/cm in 0.7% agarose gel in TBE buffer (89 mM Tris-borate, 2 mM EDTA, pH 8) during 18–24 h at room temperature. In these conditions, break yields included prompt strand breaks and breaks resulting from labile sites (Jones et al. 1994). Gels were stained in TBE buffer containing 0.5  $\mu\text{g}/\text{ml}$  ethidium bromide for 1h and destained for 1h in TBE buffer. Gel images were quantified with a fluor-S<sup>®</sup> Multimager (Bio-Rad, Hercules, CA, USA). Background was calculated as the average background above and below each DNA band. The amount of supercoiled DNA was corrected by a factor of 1.4 for the less-efficient incorporation of ethidium bromide into this plasmid form (Milligan et al. 1993). Relative amounts of the three DNA forms (supercoiled, relaxed, and linear) were calculated for each dose.

#### Bacterial survival assay

Plasmid DNA was analyzed for its efficiency to transform ampicillin-sensitive *E. coli* XL2-Blue MRF<sup>+</sup> (*recA1*) cells (Stratagene, La Jolla, CA, USA). Intact plasmids confer ampicillin resistance to the bacteria. Bacteria were made competent using the Calcium/ MOPS method (Strike et al. 1979). They were transformed by the plasmids (kept at 4°C) within a few hours to a few days after irradiation. For each dose point, 50 ng plasmid (10  $\mu\text{l}$ ) was added to a 15 ml plastic tube which contained 150  $\mu\text{l}$  of 75 mM  $\text{CaCl}_2$  and 200  $\mu\text{l}$  competent bacteria. Tubes were incubated for 45 min on ice and heat-shocked for 2 min at 42°C. Bacteria were allowed to recover for one hour at 37°C after addition of LB. For each dose, two repeats of three dilutions were plated on LB plates containing 40  $\mu\text{g}/\text{ml}$  ampicillin. The next day, colonies on each plate were counted. In most cases, plates containing between 50 and 300 colonies were used for further analysis.

#### Estimation of strand break yields

Reliable estimation of the yield of DSB requires irradiation at very high doses. At these high doses, multiple track effects (i.e. two lesions formed on the same plasmid by independent tracks) become important and the dose response curves become non-linear. In order to extract the yield of SSB and single-hit DSB, we fitted the relative amounts of supercoiled (SC), open-circular (OC) and linear (L) plasmid forms (measured with gel electrophoresis over a broad range of doses) to a mathematical model previously described by Cowan et al. (1987). As we could not reliably quantify the fragmented (F) plasmid form, we renormalized the model prediction without it. The original model contained as para-

Table I. Characteristics of the radiation types used in this study.

Irradiation type	Energy [MeV]	LET [keV $\text{mm}^{-1}$ ]	Range in $\text{H}_2\text{O}$ [cm]
$^{60}\text{Co}$	1.17, 1.33	0.267 <sup>a</sup>	$2.2 \times 10^{-2c}$
$^{137}\text{Cs}$	0.662	0.395 <sup>a</sup>	$6.4 \times 10^{-3c}$
Protons	249	0.39	$3.8 \times 10^1$
Protons	19.3	2.7	$4.0 \times 10^{-1}$
Protons	1.03	$25.5 \pm 2.3^b$	$2.6 \times 10^{-3}$
Helium	26	25.5	$5.8 \times 10^{-2}$

<sup>a</sup>Mean LET of secondary electrons, <sup>b</sup>range of LET due to energy degradation within the approximately 10 mm thick sample. range of secondary electrons of average energy produced by  $\gamma$ -rays.

measures the yields of SSB ( $\mu$ ) and DSB ( $\phi$ ) created by independent action of nicking (SSB forming) and cleaving (DSB forming) enzymes, respectively. As pointed out by Cowan et al. (1987), this model can also be used to determine the yields of SSB and DSB induced by ionizing radiation. The model distinguishes the DSB formed by single projectiles from those formed by the independent action of multiple projectiles (inducing multiple SSB on opposite strands at a distance of less than  $b \times \text{plasmid length}$  base pairs apart). The model also takes into account multiple strand breaks occurring within the same plasmid where only one is detected (e.g. a second SSB in a relaxed plasmid will not cause it to change conformation). From this model we get the following predicted yields for the various plasmid forms irradiated to a dose of  $D$ :

$$\begin{cases} SC(\mu, \phi, b, D) = e^{\phi D} e^{-\mu D} \\ OC(\mu, \phi, bn, D) = e^{-\phi D} (2e^{\mu D/2} 2e^{\mu D} + \mu DX) \\ L(\mu, \phi, b, D) \cong e^{-\phi D} \left( \frac{\mu D}{2 - b\mu D} (\mu DX - \Upsilon + e^{-\mu D/2} - e^{-\mu D}) \right. \\ \quad \left. + \phi D (e^{-\mu D} + (2e^{\mu D/2} - 2e^{\mu D} + \mu DX)) \right) \\ F(\mu, \phi, b, D) = 1 - SC(\mu, \phi, b, D) - OC(\mu, \phi, b, D) - L(\mu, \phi, b, D) \end{cases} \quad (2a)$$

with

$$\begin{cases} X = \sum_{k=1}^{\lfloor 1/b \rfloor} e^{-\mu D(1-kb)/2} \frac{[\frac{1}{2}\mu D(1-kb)]^{2k-1}}{2k!} \\ \Upsilon = \sum_{k=1}^{\lfloor 1/b \rfloor} e^{-\mu D(1-kb)/2} \left( 2k + \frac{1}{2}\mu D(1-kb) \right) \frac{[\frac{1}{2}\mu D(1-kb)]^{2k-1}}{2k!} \end{cases} \quad (2b)$$

The model-predicted yields of the various plasmid forms, normalized to  $(SC + OC + L) = 100\%$ , were fitted to the measured ones (also normalized without the fragmented fraction), taking the yield of SSB ( $\mu$ ) and DSB ( $\phi$ ) as fitting parameters and  $b = (10 \text{ bp} / 10,327 \text{ bp})$ , using the algorithm of Marquardt (1963), implemented in the Matlab software package (The MathWorks Inc., Natick, MA). We corrected for SSB existing in the plasmid pre-irradiation, by replacing  $\mu D$  with  $\mu D + \mu_0$  where  $\mu_0$  is an additional fitting parameter (the yield of SSB at zero dose). The SSB and DSB yields obtained from the fit are, therefore, the true single-track induced yields.

Correct application of Cowan's model requires knowledge of the interaction distance between strand breaks ( $b \times \text{plasmid length}$  is the maximum distance between two SSB on opposite strands that will result in a DSB). In our model calculations, we used an interaction distance of 10 bp for DSB formation, supported by the experimental values of 6–13 found by Dianov et al. (1991), Hanai et al. (1998) and D'Souza and Harrison (2003). However, we have noted that the model yielded similar results for an interaction distance of 20 bp; this indicates that the

formation of DSB by two independent SSB occurring within 10–20 bp (3–6 nm) is a rare event over the dose range investigated and could probably be neglected.

#### Estimation of clustered lesion yields

We define clustered DNA lesions as those with at least one SSB or damaged base on each of the two complementary strands, occurring within a distance of 10 bp. *In-vitro*, base excision repair of opposed base damages at a distance 2–7 bp apart can result in a DSB (for review see Blaisdell et al. 2001). In order to quantify clustered-lesions containing damaged bases *in-vivo*, we have introduced the plasmids into bacteria. As we worked with a *recA*-bacterial strain, we assumed that the clustered lesions converted into DSB were not repaired and resulted in plasmid inactivation. This assumption is supported by experimental work: two uracils on opposed strands (1–12 base apart) are converted to DSB at an efficiency of at least 80% by a bacterial repair system, whereas single uracils are not (Dianov et al. 1991; D'Souza and Harrison 2003).

Based on transformation experiments with two different plasmids conferring resistance to different antibiotics, we estimated that in our transformation assay the fraction of transformed bacteria containing more than one plasmid was less than 10%. In our analysis, we assumed that the inactivation efficiency of supercoiled and open circular plasmids was zero, while that of linear plasmids, containing one or more DSB, was one. Further, plasmids containing at least one non-DSB clustered lesion were assumed to be linearized inside the bacteria due to the action of base excision repair enzymes. Since the number of lesion clusters per plasmid is, in a good approximation, described by a Poisson distribution,  $-\ln(SF)$ , where  $SF$  is the survival fraction, was interpreted as the average number of clustered lesions per plasmid. The  $-\ln(SF)$  values were fitted to the model of Cowan et al. (1987), using the relation

$$SF(D) = \frac{SC(D) + OC(D)}{(SC + OC)_{\text{zero dose}}} \quad (3)$$

where  $SF(D)$ ,  $SC(D)$  and  $OC(D)$  are respectively the survival fraction, relative amount of supercoiled plasmids and relative amount of open-circular plasmids, at a given dose  $D$ . Using this mathematical model, we estimated the yield of single-hit clustered lesions.

It is interesting to note that the value of  $-\ln(SF)$  depends linearly on the yield of clustered lesions ( $\phi D$  in the Cowan formalism) but nonlinearly on the yield of isolated lesions ( $\mu D$ ). This can be seen by inserting equations 2 into equation 3:

$$\begin{aligned}
-\ln(SF(D)) &\propto -\ln[SC(D) + OC(D)] \\
&= -\ln \left[ e^{-\phi D} D^{-\mu D} + e^{-\phi D} \left( 2e^{-\mu D/2} - 2e^{\mu D} \right. \right. \\
&\quad \left. \left. + \mu D \sum_{j=1}^{\lfloor 1/b \rfloor} e^{-\mu D(1+jb)/2} \frac{(\frac{1}{2}\mu D(1-jb))^{2j-1}}{2j!} \right) \right] \quad (4) \\
&= \phi D - \ln(\text{complex function of } \mu D \text{ but not of } \phi D)
\end{aligned}$$

This can also be understood intuitively, as a linear dependence on dose corresponds to a single hit mechanism, while a nonlinear dependence on dose indicates that several particle traversals are required to form the endpoint under study.

Fitting Cowan's model to the log survival data as a function of dose can be used for extraction of both clustered-and single-lesion yields. The latter (single damaged bases or strand breaks) obtained from this model fit is particularly prone to errors because, as shown above, the yield of clustered lesions is manifested in the slope of the log survival curves (see Figure 5) while the yield of single lesions is manifested in its curvature. While the former can usually be extracted even with a relatively large spread of the data points, the extraction of the latter is unreliable (due probably to variability in the amount of recovered DNA).

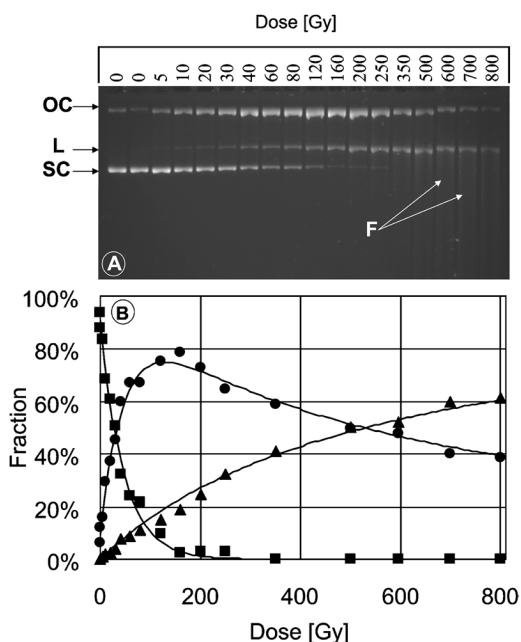


Figure 2. Evaluation of strand-break yields. (A) Migration pattern of supercoiled (SC), open-circular (OC) and linear (L) plasmid forms as function of the dose (25.5 keV/ $\mu\text{m}$  protons, 2 mM glycerol). The smeared fraction F corresponds to fragmented plasmids. (B) Fitting of the data (symbols) of (A) to the model of Cowan et al. (1987) (lines) results in experimental SSB and DSB yields of  $2.5 \cdot 10^{-9} \text{ Gy Da}^{-1}$  and  $2.5 \cdot 10^{-10} \text{ Gy}^{-1} \text{ Da}^{-1}$ , respectively. The circles correspond to the OC, the triangles to the L, the squares to the SC fractions.

We therefore do not present the single-lesion yield data.

## Results

### Strand breaks yields

Figure 2A shows an example of a gel electrophoresis of a DNA sample irradiated in 2 mM glycerol solution with  $25.5 \text{ keV } \mu\text{m}^{-1}$  protons, demonstrating the dose-variation of the main plasmid forms: The supercoiled (SC) fraction corresponds to plasmids without strand breaks, the open-circular (OC) fraction to plasmids containing one or more isolated SSB, and the linear (L) fraction to plasmids containing one or more closely spaced DSB. Multiple DSB in one plasmid result in the fragmentation of the DNA, visible as a smear (F) in the gel image.

The yield of the three fractions (SC, OC and L), as quantified from the gel image in Figure 2A, is plotted as a function of dose in Figure 2B. The amount of strand break free plasmid (SC) drops exponentially with dose as expected from Poisson statistics. The observed trend in the quantity of the open circular plasmid form (OC) is due to multiple hits on the same plasmid. At low dose, this is exceedingly rare as only a small fraction of the plasmids are damaged. As the dose increases, plasmids containing a single SSB acquire additional SSB, which does not lead to a further increase of the OC fraction. On the other hand, when a DSB is formed in a relaxed plasmid, the latter is converted to L form. This explains the observed increase of L forms accompanied by a decrease of OC forms. Furthermore, if a second SSB is formed close enough to an existing SSB (and on the opposing strand), a DSB will result. As we are interested only in single-track events, we have used the model of Cowan et al. (1987) to extract the yield of single-hit SSB and DSB from the relative intensities of each band. This model (lines in Figure 2B) describes the experimental data (symbols in Figure 2B) accurately. Using it, SSB and DSB yields were estimated for all of the radiation fields listed in Table I.

### LET and track structure dependence of SSB yields.

Figure 3 shows the SSB yield in  $\gamma$ -, proton- and helium-nucleus-irradiated plasmids as a function of LET in the range of 0.2 to  $25.5 \text{ keV } \mu\text{m}^{-1}$  for low (2 mM) and high (200 mM) glycerol scavenger concentrations, the experimental uncertainties manifest in the error bars of Figures 3–6 are explained in the appendix.

As expected, due to the longer lifetime of OH radicals at the lower scavenger concentration, the low-scavenger yields were about an order of magni-

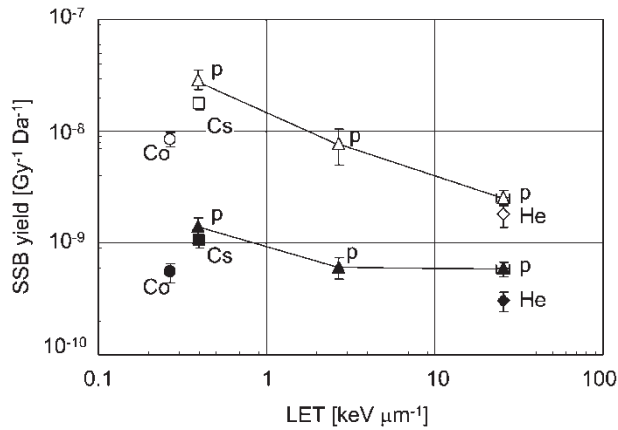


Figure 3. SSB yields as function of LET for proton (p), helium nuclei (He), <sup>60</sup>Co (Co) and <sup>137</sup>Cs (Cs). Open symbols correspond to 2 mM glycerol and closed symbols to 200 mM. The protons data are joined by a line to guide the eye. Data are the mean of 2–3 experiments except for <sup>137</sup>Cs with 200 mM glycerol (one experiment), calculated as explained in the appendix. The calculation of the error bars is also explained in the appendix.

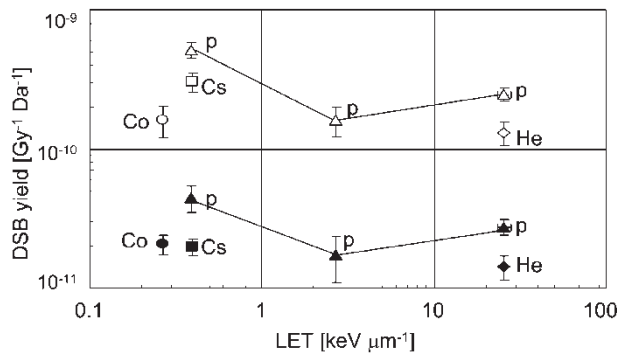


Figure 4. Yield of DSB as function of LET. Notations are the same as in Figure 3.

tude higher than the high-scavenger yields. At both glycerol concentrations, the SSB yield decreased with increasing LET although the dependence on LET was more pronounced at the lower scavenger concentration (2 mM glycerol).

Despite similar or equal LET values, the SSB yields for helium nuclei as well as that for the <sup>60</sup>Co were smaller than those for protons of 1.03 MeV and <sup>137</sup>Cs, respectively.

#### LET and track structure dependence of direct DSB yields.

Figure 4 shows the DSB yield as a function of the LET for γ-, proton-and helium-nucleus irradiations. Similar to SSB, the yield of DSB was about one order of magnitude higher at the low scavenger concentration.

At both glycerol concentrations, the DSB yield in proton-irradiated plasmids decreased between 0.39 and 2.7 keV μm<sup>-1</sup>, followed by a slight increase for

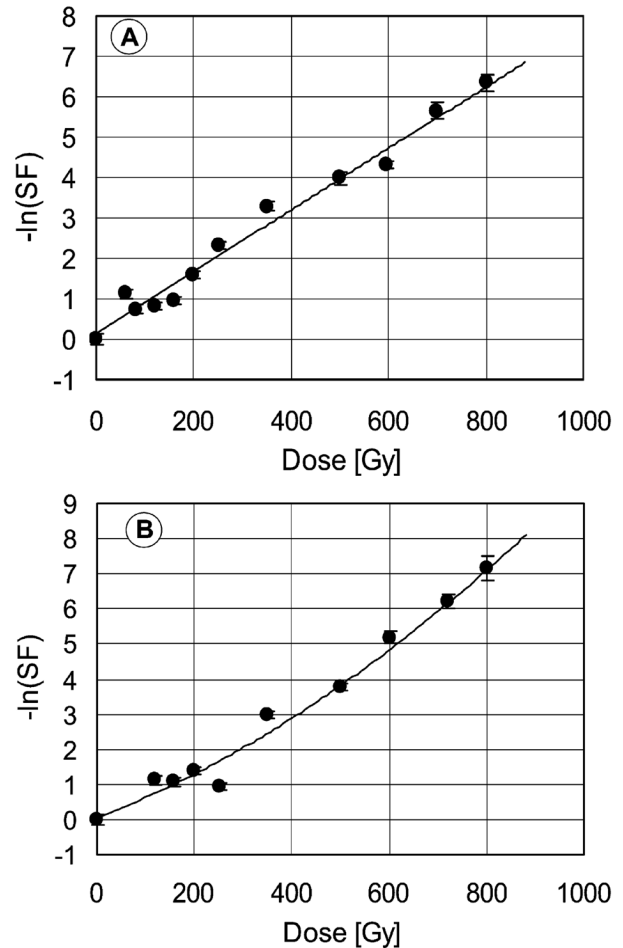


Figure 5. Survival of transformed bacteria as function of the dose. After irradiation in 2 mM glycerol solution with (A) 25.5 keV μm<sup>-1</sup> protons, (B) 2.7 keV μm<sup>-1</sup> protons. The data are presented as a negative natural logarithm for the survival fraction, -ln(SF). The symbols correspond to the measurement and the line to the model fit. The calculation of the error bars is explained in the appendix.

25.5 keV μm<sup>-1</sup> protons. The yield of DSB induced by helium nuclei of 25.5 keV μm<sup>-1</sup> was about twofold lower than that induced by protons of the same LET. The yield of DSB induced by both <sup>60</sup>Co and <sup>137</sup>Co γ-rays was also lower than that of DSB induced by 0.39 keV μm<sup>-1</sup> protons, despite their similar LET, at both glycerol concentrations. Furthermore, at 2 mM glycerol, the DSB yield was higher for <sup>137</sup>Cs irradiated plasmid compared to irradiation with <sup>60</sup>Co.

#### Clustered-lesion yields

Figure 5 shows examples for the dose-dependence of the negative natural logarithm of the survival fraction, -ln(SF), of bacteria transformed with plasmids irradiated with 25.5 keV μm<sup>-1</sup> protons (1.03 MeV) (A) and 2.7 keV μm<sup>-1</sup> protons (19.3 MeV) (B).

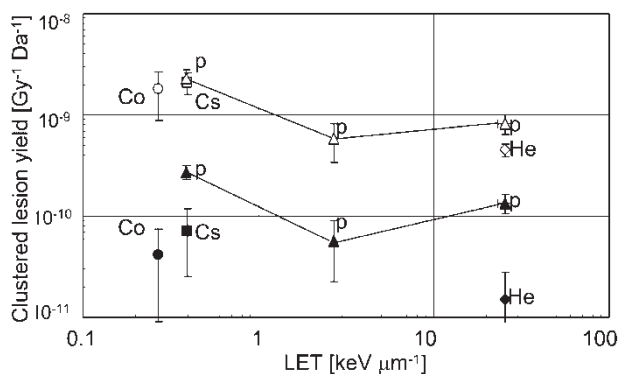


Figure 6. Yield of clustered lesions as function of the LET. Notations are the same as in Figure 3.

The shape of these curves affords some insight into the mechanism of clustered lesion formation. If the dose response is linear, clusters are formed by a “onehit” mechanism, i.e., they are caused by a single projectile. If, however, the clusters are due to the interaction of single lesions formed by several independent projectiles, the dose dependence of the yield is nonlinear with quadratic or higher-order components. Indeed, we found that the dose dependence of  $-\ln(SF)$  for  $\gamma$ -irradiation, 0.39 and 2.7 keV  $\mu\text{m}^{-1}$  protons was nonlinear whilst for the higher LET radiations (protons and helium nuclei of 25.5 keV  $\mu\text{m}^{-1}$ ), where the lesions are more clustered in nature, it was mostly linear.

Dose-survival data were fitted to Cowan’s model (Cowan et al. 1987), as described in the methods section, to determine the yield of inactivating lesions (per Gray per Dalton) which were interpreted as clustered lesions, for all of the radiation fields listed in Table I (Figure 6).

In general, the LET dependence of the clustered lesion yields (Figure 6) was similar to the LET dependence of DSB yields, albeit the absolute yields of clustered lesions were 2–8 times higher. The ratio between low- and high-scavenger clustered lesion yields was similar to that for DSB and SSB. The clustered lesion yield reached a minimum for 2.7 keV  $\mu\text{m}^{-1}$  protons. Again, at 25.5 keV  $\mu\text{m}^{-1}$  the yield was higher for protons than for helium nuclei of equal LET. On the low-LET end, 0.39 keV  $\mu\text{m}^{-1}$  protons were more effective (factor  $\sim 2$ ) in producing clustered lesions than both  $^{60}\text{Co}$  and  $^{137}\text{Cs}$   $\gamma$ -rays, principally at high scavenger concentration.

## Discussion

### LET dependence

**SSB yields.** It is well accepted that the LET dependence of the yield of SSB depends on the number of OH radicals escaping recombination.

LaVerne (1989) measured the OH radical yields produced by helium nuclei and showed that it decreases with increasing LET due to intra-track radical recombination. Using LaVerne’s data, Jones et al. (1993) showed that the SSB yield was proportional to the OH radical yield. At low scavenger concentration, the vast majority of SSB are caused by OH radicals. This explains the relatively strong decline of SSB yields between 0.39 keV  $\mu\text{m}^{-1}$  and 25.5 keV  $\mu\text{m}^{-1}$  for 2 mM glycerol (Figure 3). At the high scavenger concentration the influence of the indirect effect on SSB yields is reduced, which explains the milder decline of SSB yields.

A similar trend was found by Taucher-Scholz et al. (1992) who irradiated SV 40 DNA in solution in the LET range between 1 and 100 keV  $\mu\text{m}^{-1}$  and obtained decreasing SSB yields with a scavenging capacity of  $3.12 \times 10^7 \text{ s}^{-1}$ , a smaller decrease in yields for a capacity of  $6 \times 10^8 \text{ s}^{-1}$ , and no decrease in yields for even higher scavenging capacities, although their conclusions are based mainly on extrapolations.

**DSB and clustered lesion yields.** We investigated the LET dependence of both DSB and clustered lesions, containing breaks and/or base damages, in the LET range from 0.2 to 25.5 keV  $\mu\text{m}^{-1}$ . Over this LET range, we observed a several-fold larger yield of all clustered lesions compared to the yield of DSB, although, the general LET dependence was very similar for both yields. It should be noted that the clustered lesions we measured were of various types, ranging from 2 lesions (one SSB and one base damage on opposite strands or 2 base damages on opposite strands) to much more complex lesions (Nikjoo et al. 2001) but the bacterial transformation assay does not allow to differentiate between them. The contribution of base damages to the formation of clustered lesions and their several-fold higher yield than that of apparent DSB has also been reported by other investigators (Prise et al. 1999; Milligan et al. 2000, 2001; Sutherland et al. 2001; Gulston et al. 2002). In some cases, the transformation of base damage or abasic site into strand break is not effective, especially when the damages are one base pair apart (Blaisdell et al. 2001). Some isolated damages can also cause bacteria inactivation (Ventur and Schulte-Frohlinde 1993; Wallace 1998). Therefore the values we obtained for the clustered damage yields are influenced by these factors. However it is accepted today that the main contribution for bacteria inactivation is from clustered damages and DSB. Generally our SSB and DSB yields (see Table II and Figure 7) are consistent with previous reported data for  $^{60}\text{Co}$  (Roots et al. 1990; O’Neill et al. 1997) and  $^{137}\text{Cs}$  (Krisch et al. 1991; Milligan et

Table II. SSB (single strand break), DSB (double strand break) and CL (clustered lesion) yields after irradiation.

2 mM Glycerol					
irradiation type	LET [keV mm <sup>-1</sup> ]	SSB [10 <sup>-9</sup> Gy <sup>-1</sup> Da <sup>-1</sup> ]	DSB [10 <sup>-9</sup> Gy <sup>-1</sup> Da <sup>-1</sup> ]	CL [10 <sup>-9</sup> Gy <sup>-1</sup> Da <sup>-1</sup> ]	
$\gamma$	<sup>60</sup> Co	0.267	8.5 ± 1.3	0.16 ± 0.04	1.8 ± 0.9
Protons	<sup>137</sup> Cs	0.395	18 ± 2	0.31 ± 0.05	2.1 ± 0.5
		0.39	29 ± 6	0.52 ± 0.06	2.3 ± 0.4
		2.7	7.7 ± 3	0.16 ± 0.04	0.58 ± 0.25
He nuclei		25.5 ± 2.3a	2.6 ± 0.4	0.25 ± 0.03	0.82 ± 0.2
		25.5	1.8 ± 0.4	0.13 ± 0.02	0.45 ± 0.07
200 mM Glycerol					
$\gamma$	<sup>60</sup> Co	0.267	0.55 ± 0.1	0.027 ± 0.003	0.04 ± 0.03
Protons	<sup>137</sup> Cs	0.395	1.04 ± 0.14	0.020 ± 0.002	0.07 ± 0.05
		0.39	1.41 ± 0.3	0.045 ± 0.009	0.27 ± 0.04
		2.7	0.61 ± 0.14	0.017 ± 0.006	0.057 ± 0.03
He nuclei		25.5 ± 2.3a	0.59 ± 0.09	0.028 ± 0.003	0.13 ± 0.03
		25.5	0.30 ± 0.06	0.014 ± 0.003	0.015 ± 0.013

<sup>a</sup>Range of LET due to energy degradation within the approximately 10 mm thick sample.

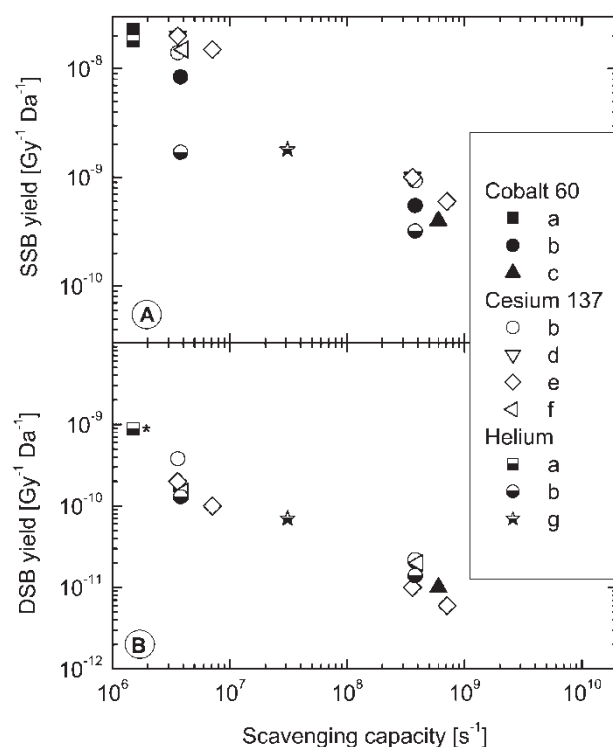


Figure 7. SSB (A) and DSB (B) yields induced by <sup>60</sup>Co, <sup>137</sup>Cs and helium nuclei irradiation. Comparison of DNA breakage yields measured by a: Roots et al. (1990) for SV40 viral DNA irradiated in 5 × 10<sup>-4</sup> M Tris-HCl, 10<sup>-4</sup> M MgCl<sub>2</sub> (LET ~16 keV μm<sup>-1</sup> according to Figure 3); b: our data; c: O'Neill et al. (1997) for plasmid irradiated in 0.1 M ethanol or 0.2 M Tris-HCl; d: Milligan et al. (1993) and e: Milligan et al. (1996b) for plasmid DNA in 10<sup>-2</sup> M sodium phosphate buffer and DMSO as scavenger; f: Krisch et al. (1991) for SV40 DNA in 0.13 M sodium chloride and 5 mM phosphate buffer with glycerol as scavenger; g: Taucher-Scholtz et al. (1999) for SV40 DNA in 10<sup>-2</sup> M Tris-HCl, 10<sup>-3</sup> M EDTA buffer (LET 26 keV μm<sup>-1</sup>). \*: DSB yields for <sup>60</sup>Co is similar to DSB yields for the helium nuclei irradiation (Roots et al. 1990).

al. 1993, 1996b). Compared to Roots et al. (1990) and Taucher-Scholtz et al. (1999), our SSB yield for irradiation with helium nuclei in presence of 2 mM glycerol seems to be low. This needs to be further investigated. To our knowledge, we are the first to have systematically investigated the LET dependence of DNA lesions in the range of 0.2–25 keV μm<sup>-1</sup> for *in-vitro* irradiation.

The LET dependence of DSB, and clustered lesions yields is determined by the following factors: (1) the number of closely spaced radicals escaping the recombination process, and (2) the overall level of clustering of radicals and direct ionizations on the DNA. These factors are modulated by the amount of scavenger present in the irradiated solution. In all radiation fields, DSB and other clustered lesions are mainly formed by local regions of higher ionization density. At low LET, these regions are widely spaced and less frequent than at higher LET. As the LET increases, they become more closely spaced and may overlap, thereby increasing the size of ionization clusters, and also of OH radical clusters. While the first effect (closer spacing) favors OH radical recombination and thereby reduces the yield of DSB, the second effect (larger size of ionization clusters) favors the production of DSB and clustered lesions. The competition between these two phenomena is probably responsible for the observed concave LET dependence of the yield of DSB and clustered lesions seen for protons.

*Adequacy of the Poisson distribution.* In our analysis, we assumed that the number of lesions per plasmid follows a Poisson distribution, however at high LET this may be not the case. For a plasmid in supercoiled shape, two regions of the double helix

can be separated by only a few nanometers. The exact shape of supercoiled DNA depends on several factors, including ionic strength, and varies from rosette-like where few regions of the double helix are in tight contact with other regions to plectonemic where the double helix interwinds for the whole length of the plasmid (Lyubchenko and Shlyakhtenko 1997). The average distance between ionization can be approximated by the ratio of the mean energy expended per ionization ( $W$  value) and the LET. This varies from 80 nm for  $0.39 \text{ KeV } \mu\text{m}^{-1}$  protons, to 1 nm for  $25.5 \text{ KeV } \mu\text{m}^{-1}$  protons and helium ions. In this case, the chance for a second hit of the plasmid by an individual  $2.7$  and  $25.5 \text{ KeV } \mu\text{m}^{-1}$  proton or helium nucleus may be higher than predicted by Poisson statistics. By assuming a Poisson distribution of the plasmid lesions, we may have underestimated the lesion yields for these irradiation fields possibly by a few tens of percent. We plan to perform irradiation experiments with fully relaxed and superhelical DNA and to adapt Cowan's model in order to address and quantify this issue.

#### Track structure effect on damage yields

As expected, LET does not uniquely describe the effectiveness of the various radiation fields; we observed track structure effects for protons and helium nuclei of same LET ( $25.5 \text{ keV } \mu\text{m}^{-1}$ ) as well as for 249 MeV protons and  $\gamma$ -rays having similar LET values.

At  $25.5 \text{ keV } \mu\text{m}^{-1}$  and for both glycerol concentrations, the DSB and total clustered-lesion yields were higher for protons than for helium nuclei (see Figures 4 and 6). This can be interpreted as a manifestation of the (radially) denser track structure of protons compared to that of helium nuclei (Paretzke 1987), leading to denser ionizations and radical formation, favoring clustered damage. Although such a difference was observed for cell death (Belli et al. 1989; Folkard et al. 1989, 1996; Goodhead et al. 1992) and mutation induction (Belli et al. 1992), this was not clearly shown for DSB yield (Jenner et al. 1992) in irradiated cells.

At  $25.5 \text{ keV } \mu\text{m}^{-1}$  and for both glycerol concentrations, the yield of SSB was twofold higher for protons than for helium nuclei (see Figure 3). This result may seem surprising, because one would expect that the denser ionization track structure of  $1.03 \text{ MeV}$  protons would cause fewer isolated lesions such as SSB. But we should remember that the gel analysis cannot distinguish between isolated SSB and lesion clusters containing an SSB and one (or more) damaged bases. The yield of this kind of clusters is indeed expected to be higher for protons than for helium nuclei due to their denser track

structure. These clustered lesions are detected by the gel assay as SSB, explaining the higher SSB yield we found.

At low LET, we have compared DNA lesion yields for  $\gamma$ -rays from  $^{60}\text{Co}$  and  $^{137}\text{Cs}$  radioactive sources and 249 MeV protons ( $0.39 \text{ keV } \mu\text{m}^{-1}$ ). Although these radiation qualities are generally considered equivalent low LET radiations, we found in some cases differences in strand break and clustered lesion yields. In general, the yields for  $^{60}\text{Co}$   $\gamma$ -rays were lower than those for  $^{137}\text{Cs}$   $\gamma$ -rays and 249 MeV protons. This may be explained by a difference in track structure between  $^{60}\text{Co}$   $\gamma$ -rays,  $^{137}\text{Cs}$   $\gamma$ -rays and 249 MeV protons. Low-LET track structures are mainly determined by the start energies of the electrons ejected in inelastic events and by the distance between subsequent inelastic collisions, which is large compared to the range of most secondary electrons. Thus, the influence of OH radical recombination on break yields (apart from at the electron track ends) should be negligible and different damage yields should reflect differences in the energy distribution of secondary electrons. The secondary electron energy spectra of  $^{60}\text{Co}$   $\gamma$ -rays,  $^{137}\text{Cs}$   $\gamma$ -rays and 249 MeV protons are clearly different. For example  $^{60}\text{Co}$   $\gamma$ -rays produce electrons with energies greater than those due to  $^{137}\text{Cs}$   $\gamma$ -radiation (e.g. Figure 3.5.b of Paretzke 1987). As high-energy electrons are known to be less effective in producing strand breaks and base damages than lower-energy ones (Nikjoo 2002a), this results in lower damage yields induced by  $^{60}\text{Co}$   $\gamma$ -rays compared to  $^{137}\text{Cs}$   $\gamma$ -rays. For clustered lesions (at both scavenger concentrations) and DSB yields (at high scavenger concentration), the difference between  $^{60}\text{Co}$  and  $^{137}\text{Cs}$  is attenuated due the recombination at the electron track ends.

Since the high damage yield caused by 249 MeV protons compared to c-irradiation and to 19.3 MeV protons and  $^{60}\text{Co}$  could also be explained by oxygen depletion for the 249 MeV proton irradiations, further irradiations with protons of intermediate energies (40–250 MeV) are underway.

As far as we know, this is the first time that a radiobiological difference between the two  $\gamma$ -ray sources ( $^{60}\text{Co}$  and  $^{137}\text{Cs}$ ) and between the  $\gamma$ -ray sources and low LET protons has been quantified with *in-vitro* DNA assays. In order to compare between different groups, SSB and DSB yields caused by irradiation with  $^{60}\text{Co}$  and  $^{137}\text{Cs}$  were plotted as function of scavenging capacity on one graph (Figure 7). We see that  $^{137}\text{Cs}$  gives higher SSB yield than  $^{60}\text{Co}$  but that this trend is not apparent for the DSB yields. Irradiating cells, Chen and Watt (1986) have seen similar magnitude variations in the reproductive survival of V79 and HeLa cells, by comparing data from several sources of  $\gamma$ -rays and

heavy ion irradiations; track structure simulations investigating this effect are under way (B. Grosswendt 2003).

Our findings demonstrate that the common notion of all  $\gamma$ -rays having the same relative biological effectiveness (RBE) may be not accurate. In consequence, one may need to take these differences into account when using different  $\gamma$ -rays as a reference radiation in radiobiology experiments.

### Summary and outlook

The yields of SSB, DSB and total clustered lesions were assessed for plasmid DNA in solution irradiated with  $^{60}\text{Co}$  and  $^{137}\text{Cs}$   $\gamma$ -rays, 1.03–249 MeV protons and 26 MeV helium nuclei. Since most previous irradiation studies with ionized particles occurred at higher LET, our results contribute to the general understanding of radiation-induced damage for particles and in the LET range relevant for proton therapy. Clustering of lesions became apparent at various levels of the analysis and was dependent on the LET of the radiation fields as well as on the track structure variations between different radiation fields of equal LET and between different  $\gamma$ -ray energies. Furthermore, we observed two unexpected effects. First, in the irradiation with protons, we observed a decrease followed by an increase for DSB and clustered damage yields as function of LET. Apparently, for an LET value of a few  $\text{keV } \mu\text{m}^{-1}$ , the effect of the cluster size per unit-energy deposited overcomes the effect of radical recombination and the DSB and complex-lesion yields slightly increase. Second, we found a difference in the results obtained with  $^{60}\text{Co}$  and  $^{137}\text{Cs}$   $\gamma$ -rays and with 0.39  $\text{keV } \mu\text{m}^{-1}$  protons, in the low-LET range of 0.2–0.4  $\text{keV } \mu\text{m}^{-1}$ , which may be explained by differences in the energy spectrum of secondary electrons in this LET range. However, these effects need to be more accurately characterized and systematic measurements of irradiating with protons at intermediate LET, between 0.39 and 2.7  $\text{keV } \mu\text{m}^{-1}$ , are under way. The difference between the  $^{60}\text{Co}$ - and  $^{137}\text{Cs}$ -induced damage yields can have consequences when calculating RBE (relative biological effectiveness) values for comparing the effects of other radiation fields, since both  $^{60}\text{Co}$  and  $^{137}\text{Cs}$  radiation fields are currently interchangeably used as references.

The results of this work may be used to validate biophysical models of radiation-induced DNA lesions. In recent years, we have developed nanodosimetry as an experimental method that provides probability distributions of ionization cluster sizes induced by radiation within a defined gas volume, simulating a 10–50 base pair DNA segment (Shchemelinin et al. 1996; Garty et al. 2002 and references therein). The measured ionization cluster

size can be related to the clustering level of radiation-induced DNA lesions using a biophysical model (Garty 2004) that correlates ion event size and DNA lesion size distributions; our data are currently used for testing this model.

### Acknowledgements

A sample of plasmid pHAZE was kindly provided to J. R. M. by Dr W. Morgan, Laboratory of Radiobiology, University of California at San Francisco. The authors are indebted to the WIS accelerator staff and especially to Y. Shachar, for their assistance with the accelerator experiments and to M. Klin for his technical assistance. We would like to thank G. Ben-Moshe and S. Ovadia of the WIS  $\text{c}$ -irradiation facility for their cooperation during long irradiations, the WIS bacteriology unit for their supportive collaboration in the bacterial survival experiments and G. Heyes for useful advice. We would also like to thank Y. Shrot for his assistance with the assembly and characterization of the beam dosimetry system. S. S. is supported by the state of Israel, the Ministry of Absorption and the Center for Absorption of Scientists. A. B. is the W. P. Reuther Professor of Research in the peaceful uses of Atomic Energy. J. R. M. was supported by the UCSD Cancer Center, National Institutes of Health grant CA46295, and the National Aeronautics and Space Administration (NCCW-98). This work was partially supported by the National Medical Technology Testbed Inc. (NMTB) under the US Department of the Army Medical Research Acquisition Activity, Cooperative Agreement Number DAMD17-97-2-7016 and by the MINERVA Foundation. The views, opinions and/or findings contained in this report are those of the authors and should not be construed as a position, policy, decision or endorsement of the US Federal Government and NMTB.

### References

- Ayene IS, Koch CJ, Krisch RE, 1995. Role of scavenger-derived radicals in the induction of double-strand and single-strand breaks in irradiated DNA. *Radiation Research* 142: 133–143.
- Bashkirov V, Schulte RW, 2002. Dosimetry system for the irradiation of thin biological samples with therapeutic proton beams. *Physics in Medicine and Biology* 47: 409–420.
- Belli M, Cherubini R, Finotto S, Moschini G, Sapora O, Simone G, Tabocchini MA, 1989. RBE-LET relationship for the survival of V79 cells irradiated with low energy protons. *International Journal of Radiation Biology* 55: 93–104.
- Belli M, Goodhead DT, Ianzini F, Simone G, Tabocchini MA, 1992. Direct comparison of biological effectiveness of protons and alpha-particles of the same LET. II. Mutation induction at the HPRT locus in V79 cells. *International Journal of Radiation Biology* 61: 625–629.

- Belli M, Ianzini F, Saporà O, Tabocchini MA, Cera F, Cherubini R, Haque AM, Moschini G, Tiveron P, Simone G, 1996. DNA double strand break production and rejoining in V79 cells irradiated with light ions. *Advances in Space Research* 18: 73–82.
- Belli M, Cherubini R, Dalla Vecchia M, Dini V, Esposito G, Moschini G, Saporà O, Simone G, Tabocchini MA, 2002. DNA fragmentation in V79 cells irradiated with light ions as measured by pulsed-field gel electrophoresis. I. Experimental results. *International Journal of Radiation Biology* 78: 475–482.
- Berger MJ, 1995. ESTAR, PSTAR and ASTAR: Computer programs for calculating stopping powers and ranges for electrons, protons and helium ions. In: IAEA TECDOC 799: Atomic and molecular data for radiotherapy and radiation research. Vienna: International Atomic Energy Agency. pp. 723–740.
- Bernhardt PH, Friedland W, Meckbach R, Jacob P, Paretzke HG, 2002. Monte Carlo simulation of DNA damage by low LET radiation using inhomogeneous higher order DNA targets. *Radiation Protection Dosimetry* 99: 203–206.
- Blaisdell JO, Harrison L, Wallace SS, 2001. Base excision repair processing of radiation-induced clustered DNA lesions. *Radiation Protection Dosimetry* 97: 25–31.
- Chapman JD, Reuvers AP, Borsa J, Greenstock CL, 1973. Chemical radioprotection and radiosensitization of mammalian cells growing in vitro. *Radiation Research* 56: 291–306.
- Chen CZ, Watt DE, 1986. Biophysical mechanism of radiation damage to mammalian cells by X- and  $\gamma$ -rays. *International Journal of Radiation Biology* 49: 131–142.
- Christensen RC, Tobias CA, Taylor WD, 1972. Heavy-ion-induced single- and double-strand breaks in WX-174 replicative form DNA. *International Journal of Radiation Biology and related studies in Physics, chemistry and Medicine* 22: 457–477.
- Cowan R, Collis CM, Grigg GW, 1987. Breakage of double-stranded DNA due to single-stranded nicking. *Journal of Theoretical Biology* 127: 229–245.
- Dianov GL, Timchenko TV, Sinitina OI, Kuzminov AV, Medvedev OA, Salganik RI, 1991. Repair of uracil residues closely spaced on the opposite strands of plasmid DNA results in double-strand break and deletion formation. *Molecular and General Genetics* 225: 448–452.
- D'Souza DI, Harrison L, 2003. Repair of clustered uracil DNA damage in *Escherichia Coli*. *Nucleic Acids Research* 31: 4573–4581.
- Folkard M, Prise KM, Vojnovic B, Davies S, Roper MJ, Michael BD, 1989. The irradiation of V79 mammalian cells by protons with energies below 2 MeV. Part I: Experimental arrangement and measurements of cell survival. *International Journal of Radiation Biology* 56: 221–237.
- Folkard M, Prise KM, Vojnovic B, Newman HC, Roper MJ, Michael BD, 1996. Inactivation of V79 cells by low-energy protons, deuterons and helium-3 ions. *International Journal of Radiation Biology* 69: 729–738.
- Friedland W, Bernhardt P, Jacob P, Paretzke HG, Dingfelder M, 2002. Simulation of DNA damage after proton and low LET irradiation. *Radiation Protection Dosimetry* 99: 99–102.
- Friedland W, Jacob P, Bernhardt P, Paretzke HG, Dingfelder M, 2003. Simulation of DNA damage after proton irradiation. *Radiation Research* 159: 401–410.
- Garty G, Shchemelinin S, Breskin A, Chechik R, Assaf G, Orion I, Bashkirov V, Schulte R, Grosswendt B, 2002. The performance of a novel ion-counting nanodosimeter. *Nuclear Instruments and Methods in Physics Research A* 492: 212–235.
- Garty G, 2004. Development of ion-counting nanodosimetry and evaluation of its relevance to radiation biology, Ph.D. Thesis.
- Goodhead DT, Belli M, Mill AJ, Bance DA, Allen LA, Hall SC, Ianzani F, Simone G, Stevens DL, Stretch A, 1992. Direct comparison between protons and alpha-particles of the same LET: I. Irradiation methods and inactivation of asynchronous V79, HeLa and C3H 10T1/2 cells. *International Journal of Radiation Biology* 61: 611–624.
- Grosswendt B, 2003. Personal communication.
- Gulston M, Fulford J, Jenner T, Delara C, O'Neill P, 2002. Clustered DNA damage induced by c radiation in human fibroblasts (HF19), hamster (V79-4) cells and plasmid DNA is revealed as Fpg and Nth sensitive sites. *Nucleic Acids Research* 30: 3464–3472.
- Hanai R, Yazu M, Hieda K, 1998. On the experimental distinction between ssbs and dsbs in circular DNA. *International Journal of Radiation Biology* 73: 475–479.
- ICRU 1998, Clinical proton dosimetry part I, Beam production, beam delivery and measurement of absorbed dose. ICRU 59. Bethesda: International Commission on Radiation Units and Measurements. pp. 18–28.
- Jenner TJ, Belli M, Goodhead DT, Ianzini F, Simone G, Tabocchini MA, 1992. Direct comparison of biological effectiveness of protons and alpha-particles of the same LET. III. Initial yield of DNA double-strand breaks in V79 cells. *International Journal of Radiation Biology* 61: 631–637.
- Jones GDD, Milligan JR, Ward JF, Calabro-Jones PM, Aguilera JA, 1993. Yield of strand breaks as a function of scavenger concentration and LET for SV40 irradiated with  $^4\text{He}$  ions. *Radiation Research* 136: 190–196.
- Jones GDD, Boswell TV, Ward JF, 1994. Effects of postirradiation temperature on the yields of radiation-induced single- and double-strand breakage in SV40 DNA. *Radiation Research* 138: 291–296.
- Klimczak U, Ludwig DC, Mark F, Rettberg P, Schulte-Frohlinde D, 1993. Irradiation of plasmid and phage DNA in water-alcohol mixtures: strand breaks and lethal damage as a function of scavenger concentration. *International Journal of Radiation Biology* 64: 497–510.
- Krisch RE, Flick MB, Trumbore CN, 1991. Radiation chemical mechanisms of single- and double-strand break formation in irradiated SV40 DNA. *Radiation Research* 126: 251–259.
- Laverne JA, 1989. The production of OH radicals in the radiolysis of water with  $^4\text{He}$  ions. *Radiation Research* 118: 201–210.
- Lutze LH, Winegar RA, 1990. pHAZE: a shuttle vector system for the detection and analysis of ionizing radiation-induced mutations. *Mutation Research* 245: 305–310.
- Lyubchenko YL, Shlyakhtenko LS, 1997. Visualization of supercoiled DNA with atomic force microscopy *in situ*. *Proceedings of the National Academy of Sciences of the USA* 94: 496–501.
- Marquardt D, 1963. An Algorithm for Least Squares Estimation of Nonlinear Parameters. *SIAM Journal of Applied Mathematics* 11: 431–441.
- Milligan JR, Aguilera JA, Ward JF, 1993. Variation of single-strand break yield with scavenger concentration for plasmid DNA irradiated in aqueous solution. *Radiation Research* 133: 151–157.
- Milligan JR and Ward JF, 1994. Yield of single-strand breaks due to attack on DNA by scavenger-derived radicals. *Radiation Research* 137: 295–299.
- Milligan JR, Ng JY-Y, Wu CCL, Aguilera JA, Ward JF, Kow YW, Wallace SS, Cunningham RP, 1996a. Methylperoxyl radicals as intermediates in the damage to DNA irradiated in aqueous dimethyl sulfoxide with gamma rays. *Radiation Research* 146: 436–443.
- Milligan JR, Aguilera JA, Wu CCL, Ng JY-Y, Ward JF, 1996b. The difference that linear energy transfer makes to precursors of DNA strand breaks. *Radiation Research* 145: 442–448.

- Milligan JR, Aguilera JA, Nguyen T-TD, Paglinawan RA, Ward JF, 2000. DNA strand-break yields after post-irradiation incubation with base excision repair endonucleases implicate hydroxyl radical pairs in double-strand break formation. *International Journal of Radiation Biology* 76: 1475–1483.
- Milligan JR, Aguilera JA, Paglinawan RA, Ward JF, Limoli CL, 2001. DNA strand break yields after post-high LET irradiation incubation with endonuclease-III and evidence for hydroxyl radical clustering. *International Journal of Radiation Biology* 77: 155–164.
- Nikjoo H, O'Neill P, Terrissol M, Goodhead DT, 1999. Quantitative modeling of DNA damage using Monte Carlo track structure method. *Radiation and Environmental Biophysics* 38: 31–38.
- Nikjoo H, O'Neill P, Wilson WE, Goodhead DT, 2001. Computational approach for determining the spectrum of DNA damage induced by ionizing radiation. *Radiation Research* 156: 577–583.
- Nikjoo H, Bolton CE, Watanabe R, Terrissol M, O'Neill P, Goodhead DT, 2002a. Modeling of DNA damage induced by energetic electrons (100 eV to 100 keV). *Radiation Protection Dosimetry* 99: 77–80.
- Nikjoo H, Goorley T, Fulford J, Takakura K, Ito T, 2002b. Quantitative analysis of the energetics of DNA damage. *Radiation Protection Dosimetry* 99: 91–98.
- O'Neill P, Cunniffe SMT, Stevens DL, Botchway SW, Nikjoo H, 1997. Strand break induction in DNA by aluminium K ultrasoft X-rays: comparison of experimental data and track structure analysis. In: Goodhead, D., O'Neill, P. and Menzel, H. (Eds), *Microdosimetry An Interdisciplinary approach*. Cambridge: The Royal Society of Chemistry. pp. 81–84.
- Paretzke HG, 1987. Radiation track structure theory. In: Kase KR, Bjarngaard BE, Attix FH, editors. *The Dosimetry of Ionizing Radiation*. Vol. II. Orlando: Academic Press. pp. 89–170.
- Pastwa E, Neumann RD, Mezhevaya K, Winters TA, 2003. Repair of radiation-induced DNA double-strand breaks is dependent upon radiation quality and the structural complexity of double-strand breaks. *Radiation Research* 159: 251–261.
- Prise KM, Ahnstrom G, Belli M, Carlsson J, Frankenberg D, Kiefer J, Lobrich M, Michael BD, Nygren J, Simone G, Stenleröw B, 1998. A review of dsb induction data for varying quality radiations. *International Journal of Radiation Biology* 74: 173–184.
- Prise KM, Pullar CH, Michael BD, 1999. A study of endonuclease III-sensitive sites in irradiated DNA: detection of alpha-particle-induced oxidative damage. *Carcinogenesis* 20: 905–909.
- Prise KM, Pinto M, Newman HC, Michael BD, 2001. A review of studies of ionizing radiation-induced double-strand break clustering. *Radiation Research* 156: 572–576.
- Roots R, Holley W, Chatterjee A, Irizarry M, Kraft G, 1990. The formation of strand breaks in DNA after high-LET irradiation: a comparison of data from *in vitro* and cellular systems. *International Journal of Radiation Biology* 58: 55–69.
- Rydberg B, 2001. Radiation-induced DNA damage and chromatin structure. *Acta Oncologica* 40: 682–685.
- Shchemelinin S, Breskin A, Chechik R, Pansky A, Colautti P, Conte V, De Nardo L, Tornielli G, 1996. Ionization measurements in small gas samples by single ion counting. *Nuclear Instruments and Methods in Physics Research A* 368: 859–861.
- Spinks JWT, Woods RJ, 1976. *An introduction to radiation chemistry*, 2nd ed. New York: Wiley. p. 93.
- Strike P, Humphreys GO, Roberts RJ, 1979. Nature of transforming deoxyribonucleic acid in calcium-treated *Escherichia coli*. *Journal of Bacteriology* 138: 1033–1035.
- Sutherland BM, Bennett PV, Schenk H, Sidorkina O, Laval J, Trunk J, Monteleone D, Sutherland J, 2001. Clustered DNA damages induced by high and low LET radiation, including heavy ions. *Physica Medica* 17(Supplement 1): 202–204.
- Taucher-Scholz G, Stanton JA, Schneider M, Kraft G, 1992. Induction of DNA breaks in SV40 by heavy ions. *Advances in Space Research* 12: (2)73–(2)80.
- Taucher-Scholz G, Kraft G, 1999. Influence of radiation quality on the yield of DNA strand breaks in SV40 DNA irradiated in solution. *Radiation Research* 151: 595–604.
- Ventur Y, Schulte-Frohlinde D, 1993. Does the enzymatic conversion of DNA single-strand damage into double-strand breaks contribute to biological inactivation of c-irradiated plasmid DNA? *International Journal of Radiation Biology* 63: 167–171.
- Wallace SS, 1998. Enzymatic processing of radiation-induced free radical damage in DNA. *Radiation Research* 150(supplement): S60–S79.
- Ward JF, 1988. DNA damage produced by ionizing radiation in mammalian cells: identities, mechanisms of formation, and reparability. *Progress in Nucleic Acid Research and Molecular Biology* 35: 95–125.
- Watanabe R, Saito K, 2002. Monte Carlo simulation of strand-break induction on plasmid DNA in aqueous solution by monoenergetic electrons. *Radiation and Environmental Biophysics* 41: 207–215.

## Appendix A: Uncertainty analysis

The experimental uncertainties determining the error bars of Figures 3–6 are due to several factors. We evaluate the systematic uncertainties, which arise from the dosimetry and the sample analysis. The “stochastic” uncertainties were evaluated by repeating the experiment three times under identical conditions and calculating the standard error. Finally, we describe our method for obtaining the uncertainty in the evaluated yield of single-strand breaks, double-strand breaks and clustered lesions.

## Experimental uncertainties

**Dosimetry.** The principal uncertainty in the accelerator dosimetry is due to an uncertainty in the thickness and pressure of the ionization chamber. The ionization chamber thickness was  $1.6 \pm 0.1$  mm (6%). It was operated at atmospheric pressure, which could vary by up to 5%. Other factors included in the dose calculation (temperature,  $w_i$  value, beam area, etc) are known to better than 1%. The uncertainty in the dose evaluation, determined by the uncertainty in IC thickness and the gas density, is therefore 8%.

The uncertainty in the dosimetry of the c-irradiations was quantified by comparing the slopes of the optical density of an irradiated Fricke solution as a function of the nominal dose. The standard deviation of 8 such slopes measured at different dates and using different Fricke solutions was 9%.

*Possible uncertainties stemming from the irradiation protocol.* A great effort was put to verify that our irradiation protocol does not result in a significant yield of damages to the irradiated DNA, beyond those induced by the particle radiation field. In particular we have seen that (a) the weak proton-induced activation of the quartz substrate does not induce a noticeable quantity of additional SSB or DSB compared to an irradiation of the same duration, by the same radiation field; (b) the storage of the DNA as a thin film within the sample holder for up to 8h (at room temperature) does not induce a significant quantity of SSB or DSB.

*Uncertainties in the gel analysis.* The experimental uncertainties inherent in the analysis of the gel data are due to the quantification of the band intensity and the varying binding efficiency of ethidium bromide to the various forms of DNA. The band intensity was calculated by subtracting the number of expected background counts within the band area from the number of counts in the band ( $N_{band} = N_{tot} - N_{BG}$ ). The uncertainty in this number is , which in our case is about 1%. The binding efficiency of ethidium bromide to supercoiled DNA is 1.3–1.5 times smaller than to the other forms. We have used an average value of 1.4; a change by  $\pm 0.1$  affects the fitted values by less than 5%.

A free parameter in the Cowan model is the distance between two SSB required to form a DSB ( $b \times \text{plasmid length}$ ), which was set equal to 10 bp. Its variation by  $\pm 3$  bp (corresponding to the values given by Dianov et al. (1991), Hanai et al. (1998) and D'souza and Harrison (2003)) resulted in a variation of a few  $\theta$  in the resulting fit parameters.

*Uncertainties in the bacterial survival assay.* The main uncertainty in this assay is the reproducibility of the

amount of DNA recovered from the irradiation holder and used in the transformation. This amount was seen to be slightly different for each measured dose-point, resulting in a poorer quality model fit as compared to the gel data. The stochastic uncertainty in the number of colonies on each dish was taken into account by averaging the number of counts on several dishes (weighted by the quantity  $1/\sqrt{n}$ ) of different dilutions. The error bars, shown in Figure 5, represent the average of  $1/\sqrt{n}$  of all dishes at the same dose-point.

#### *The total uncertainty*

The uncertainty in the fitted model parameters, resulting from the uncertainty in the experimental quantities, was obtained by a Monte-Carlo error propagation algorithm: For each irradiation experiment (consisting of one repetition of 10–20 dose points, as described in the text) 1000 data sets were generated by overlaying a Gaussian experimental error onto an actual data set. In the gel analysis we took the standard deviation of this distribution to be 5% of the measured yield of supercoiled, relaxed or linear DNA. In the analysis of the survival data we took the error as described in the previous paragraph. The fitting procedure was then performed to obtain the various lesion yields (SSB, DSB or clustered lesion) for each of the 1000 data sets. The experimental value for each irradiation experiment was taken as the average of these (1000) lesion yields; the experimental uncertainty was taken as their standard deviation.

The value plotted in Figures 3, 4 and 6 is the average, over all repetitions (typically 2–3) of the same radiation field, of the experimental value calculated above. The error bars are obtained by adding (in quadrature) the uncertainty in dose (8%), the standard deviation of the three repetitions and the experimental uncertainty, described in the previous paragraph and averaged (also in quadrature) over all repetitions of the same radiation field.